J Mater Sci (2008) 43:1175–1179
DOI 10.1007/s10853-007-2300-8

Estimation of lattice strain in nanocrystalline silver from X-ray diffraction line broadening

V. Biju · Neena Sugathan · V. Vrinda · S. L. Salini

Received: 17 May 2007 / Accepted: 5 November 2007 / Published online: 4 December 2007

Abstract The lattice strain contribution to the X-ray diffraction line broadening in nanocrystalline silver samples with an average crystallite size of about 50 nm is studied using Williamson-Hall analysis assuming uniform deformation, uniform deformation stress and uniform deformation energy density models. It is observed that the anisotropy of the crystallite should be taken into account, while separating the strain and particle size contributions to line broadening. Uniform deformation energy density model is found to model the lattice strain appropriately. The lattice strain estimated from the interplanar spacing data are compared with that estimated using uniform-energy density model. The lattice strain in nanocrystalline silver seems to have contributions from dislocations over and above the contribution from excess volume of grain boundaries associated with vacancies and vacancy clusters.

V. Biju
Department of Physics, Government Polytechinc College, Perumbavoor, Ernakulam, Kerala 683 544, India

Present Address:
V. Biju (✉)
Department of Physics, University of Kerala, Kariavattom Campus, Thiruvananthapuram, Kerala 695 581, India
e-mail: bijunano@yahoo.co.in

N. Sugathan
Departmet of Physics, Government College for Women, Thiruvananthapuram, Kerala 695 014, India

V. Vrinda · S. L. Salini
Department of Physics, Sree Narayana College, Kollam, Kerala 691 001, India

Introduction

Modified physical properties of nanocrystalline materials are mostly attributed to the very large percentage of interfacial region with a modified microstructure. However, recent experiments have concluded that the lattice strain in nanocrystalline samples also significantly contributes to the modified physical properties [1–3]. Previously, the lattice strain in nanocrystalline samples was attributed to the grain-interior dislocations [4, 5] and grain-boundary dislocations [6]. Recently Quin and Szpunar had traced the origin of lattice strain to the stress field due to the excess volume of grain boundaries associated with vacancies and vacancy clusters [1]. The mean magnitude of the local lattice strains in nanocrystalline samples could be estimated from the X-ray diffraction pattern using different analytical procedures. Though the full pattern fitting methods are more rigorous, the analysis involved is quite complex and hence less direct methods such as Warren-Averbach analysis or Williamson-Hall analysis is often employed. Warren-Averbach analysis requires at least two reflections along the same crystallographic direction and when higher angle reflections are weak and difficult to analyze Williamson-Hall method is preferred. This article reports a study of lattice strain in nanocrystalline silver from the X-ray diffraction pattern using Williamson-Hall analysis taking into account the anisotropy of the crystallites.

Experimental

Nanocrystalline silver (Ag) was synthesized through a wet chemical route using silver nitrate and sodium citrate as the starting materials. Transmission electron micrograph

(TEM) and Selected Area Electron Diffraction (SAED) patterns of the sample were recorded using a JEOL-JEM-2010.EX electron microscope. X-ray diffraction pattern of the sample was recorded using a Rigaku DIMAX-B, USA X-ray powder diffractometer using Copper K_α ($\lambda = 1.540598$ Å) radiation. The diffraction patterns were recorded in the range $2\theta = 20$–$80°$.

Results and discussion

Figure 1 shows the TEM image of the nanocrystalline Ag sample together with the SAED pattern. The nanocrystalline nature of the sample is clear from the TEM image. The particle size distribution is shown in Fig. 2. The mean size estimated from the TEM image is about 51 ± 8 nm. The spotty nature of the SAED pattern is in agreement with the quite wide size distribution in the sample.

X-ray diffraction pattern of the nanocrystalline silver sample is shown in Fig. 3(a). Peak positions, 2θ and full width at half maximum, $(\beta_{hkl})_{\text{measured}}$ of the Bragg peaks were determined by a self-consistent profile fitting technique using a regular Pearson VII function which assumes that the peak shape is symmetrical. Although a split Pearson VII function is known to provide better fits, the simpler function was used to limit the number of variables [7, 8]. The best-fit results were chosen taking into account the minimum error as well as realistic values for the fitting parameters. The result of the curve fit routine for the (111) peak is shown in Fig. 3(b).

In order to determine the instrumental contribution to line broadening, the diffraction pattern of the instrumental standard Silicon (Si) sample, which contributes no sample related line broadening was recorded. The instrumental setup was identical in every respect to that used for recording the diffraction pattern of nanocrystalline silver.

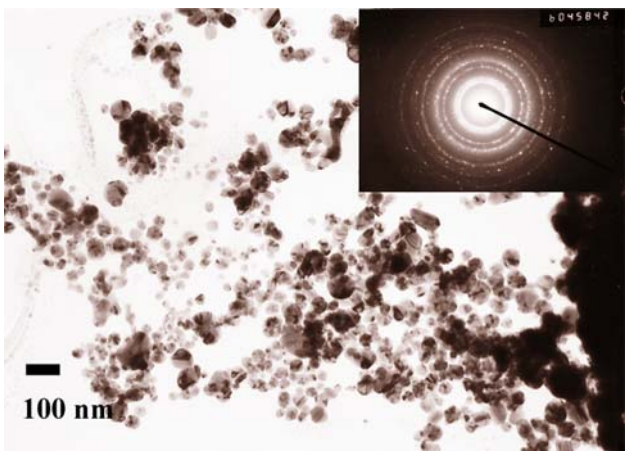

Fig. 1 TEM image and SAED pattern of nanocrystalline silver

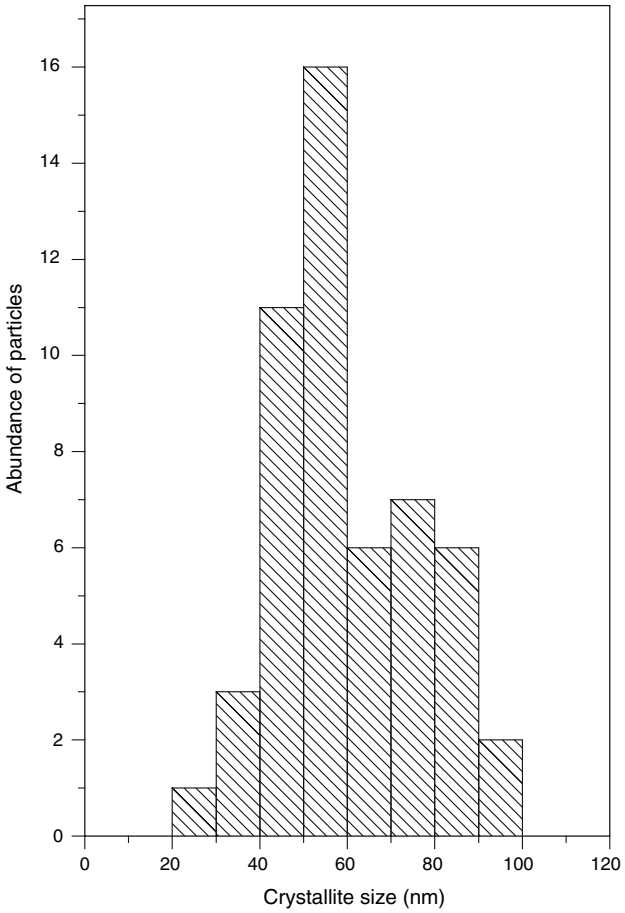

Fig. 2 Particle size distribution of nanocrystalline silver sample

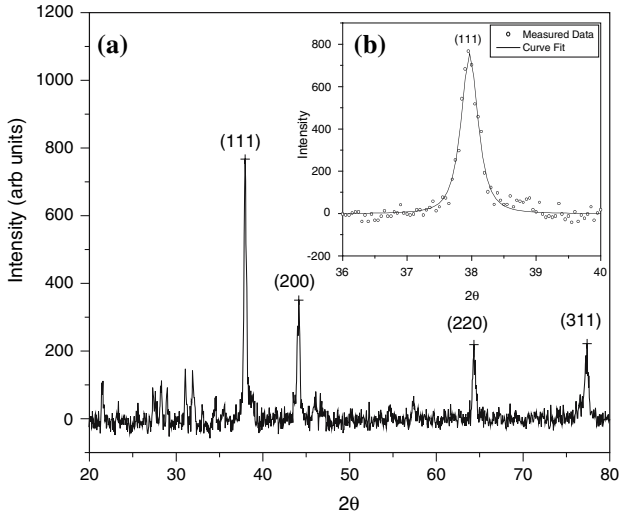

Fig. 3 (**a**) X-ray diffraction pattern of nanocrystalline silver and (**b**) results of the curve fit routine for the (111) peak

The instrumental corrected broadening, (β_{hkl}) corresponding to each diffraction peak of nanocrystalline silver was estimated using the relation

$$\beta_{hkl} = \left[(\beta_{hkl})^2_{\text{measured}} - \beta^2_{\text{instrumental}}\right]^{0.5} \quad (1)$$

In Williamson-Hall method [9, 10] it is assumed that the line broadening β_t of a Bragg reflection (h k l) originating from the small crystallite size follows Scherrer equation $\beta_t = K\lambda/t \cos\theta_{hkl}$. Here K is the shape factor, λ is the X-ray wavelength, θ_{hkl} is the Bragg angle and t is the effective crystallite size normal to the reflecting planes. Also, the strain induced broadening β_ε is given by the Wilson formula as $\beta_\varepsilon = 4\varepsilon\tan\theta_{hkl}$. Here $\boldsymbol{\varepsilon}$ is the root mean square value of the microstrain. Assuming that the particle size and strain contributions to line broadening are independent of each other and both have a Cauchy-like profile, the observed line breadth is simply the sum of the two i.e. $\beta_{hkl} = \beta_t + \beta_\varepsilon = [K\lambda/t\cos\theta_{hkl}] + [4\varepsilon\tan\theta_{hkl}]$

$$\beta_{hkl}\cos\theta_{hkl} = [K\lambda/t] + [4\varepsilon\sin\theta_{hkl}] \quad (2)$$

Equation 2 is the Williamson-Hall equation. Plotting the value of $\beta_{hkl}\cos\theta_{hkl}$ as a function of 4 sin θ_{hkl} the microstrain ε may be estimated from the slope of the line and the crystallite size from the intersection with the vertical axis. β_{hkl} value used here is the instrumental corrected values.

In the present study, Williamson-Hall analysis of nanocrystalline silver data was carried out assuming three different models, viz. uniform deformation, uniform deformation stress and uniform deformation energy density [11]. The uniform deformation model does not take into account the anisotropic nature of the crystal. Here the microstrain ε is assumed to be uniform in all crystallographic directions. The Williamson-Hall plot assuming uniform deformation model is shown in Fig. 4(a). Uniform

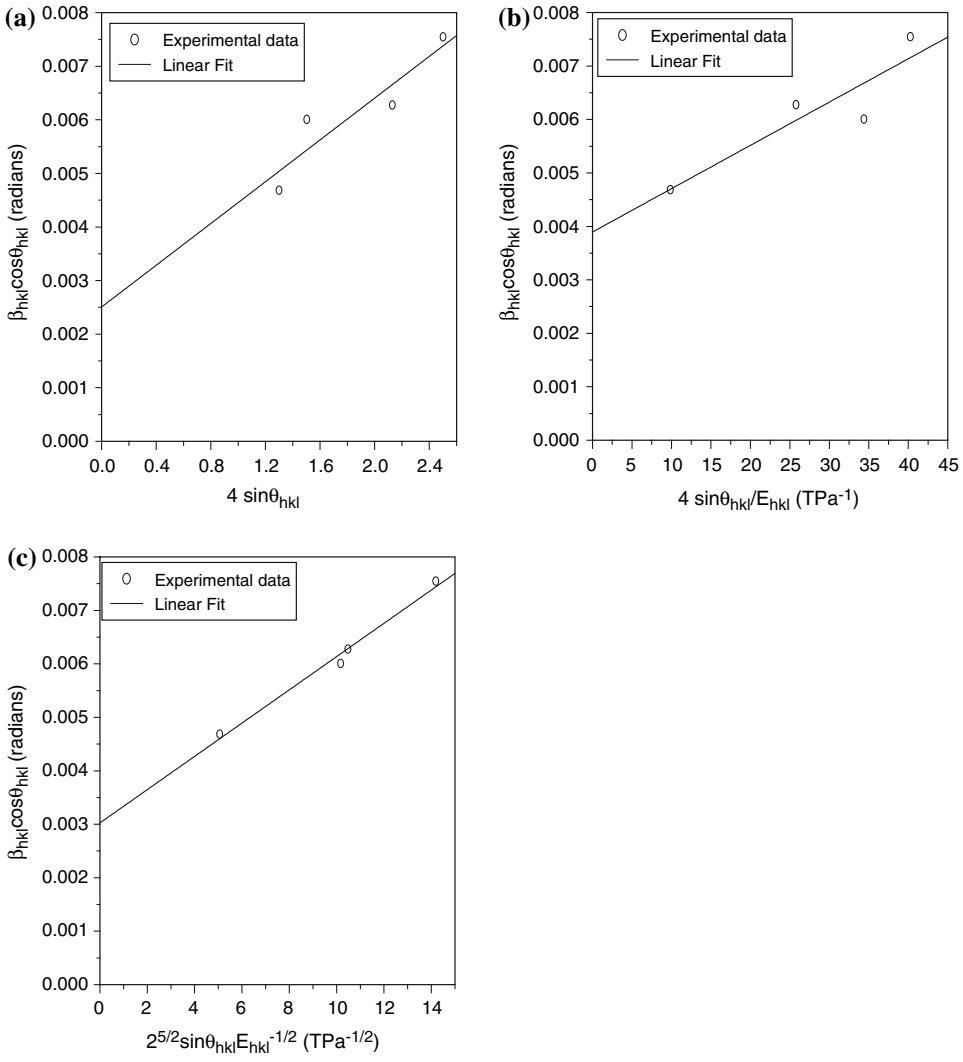

Fig. 4 Williamson-Hall plot of nanocrystalline silver sample assuming (**a**) uniform deformation model (**b**) uniform deformation stress model and (**c**) uniform deformation energy density model

deformation stress and uniform deformation energy models take into account the anisotropic nature of Young's modulus of the crystals and are hence more realistic [11]. In the uniform deformation stress model, the cause of anisotropic microstrain ε_{hkl} is assumed to be a uniform deformation stress σ. In this approach the Williamson-Hall equation has the form

$$\beta_{hkl}\cos\theta_{hkl} = [K\lambda/t] + [4\sigma\sin\theta_{hkl}/E_{hkl}] \quad (3)$$

The isotropic microstrain ε in uniform deformation model is replaced by $\varepsilon_{hkl} = \sigma/E_{hkl}$, where E_{hkl} is the Young's modulus in the direction perpendicular to the set of planes ($h\,k\,l$). Plotting the value of $\beta_{hkl}\cos\theta_{hkl}$ as a function of 4 sin θ_{hkl}/E_{hkl} the uniform deformation stress σ can be estimated from the slope of the line and the anisotropic microstrain ε_{hkl} can be calculated if the E_{hkl} values for the sample are known. Further, the crystallite size can be estimated from the intersection with the vertical axis. For cubic crystals, Young's modulus E_{hkl} in the direction perpendicular to the set of planes ($h\ k\ l$) has the form $E_{hkl} = s_{11} - (2s_{11} - 2s_{12} - s_{44})[(k^2l^2 + l^2h^2 + h^2k^2)/(h^2 + k^2 + l^2)^2$ [12]. Here s_{11}, s_{12} and s_{44} are elastic compliances. The values of s_{11}, s_{12} and s_{44} for cubic phase of silver are 22.9×10^{-12}, 22.1×10^{-12} and -9.8×10^{-12} m^2 N^{-1}, respectively [13]. The Williamson-Hall plot assuming uniform deformation stress model is shown in Fig. 4(b). In the uniform deformation energy density model, the cause of lattice strain is assumed to be a density of deformation energy u. Thus, assuming the density to be uniform, according to Hooke's law, $u = \varepsilon_{hkl}^2 E_{hkl}/2$. Therefore, Williamson-Hall equation is to be modified as:

$$\beta_{hkl}\cos\theta_{hkl} = [K\lambda/t] + \left[4(2/E_{hkl})^{1/2}\sin\theta_{hkl}\right]u^{1/2} \quad (4)$$

The Williamson-Hall plot assuming uniform deformation energy model is shown in Fig. 4(c). Here, $\beta_{hkl}\cos\theta_{hkl}$ is plotted as a function of ($2^{5/2}\sin\theta_{hkl}E_{hkl}^{-1/2}$). The uniform deformation energy density u can be estimated from the slope of the line and the anisotropic microstrain ε_{hkl} can be calculated knowing E_{hkl} values for the sample. Further, as in the previous cases, the crystallite size can be estimated from the intersection with the vertical axis. From Eqs. 3 and 4, the deformation stress and deformation energy density are related as $u = \sigma^2/E_{hkl}$. It may be noted that though both Eqs. 3 and 4 takes into account the anisotropic nature of the elastic constant, they are essentially different. This is because in Eq. 3 it is assumed that the deformation stress σ has the same value in all crystallographic directions allowing u to be anisotropic, while Eq. 4 is developed assuming the deformation energy to be uniform in all crystallographic directions treating the deformation stress σ to be anisotropic. Thus it is clear that Williamson-Hall plots using Eqs. 3 and 4 for a given sample may result in different values for lattice strain and crystallite size. For a given sample, Williamson-Hall plots may be plotted using Eqs. 1–3 and the most suitable model may be chosen as the one which result in the best fit of the experimental data.

A comparison of the three evaluation procedures for nanocrystalline Ag sample is possible from the analysis of Fig. 4(a–c). The scattering of the points away from the linear expression is much less for part (c) in comparison with parts (a) and (b). Further, the average crystallite sizes estimated from the Y-intercept of the graphs in Fig. 4(a–c) are respectively 61.39, 39.51 and 50.86 nm respectively. It can be noted that the value of the average crystallite size obtained from the uniform deformation energy model (Fig. 4(c)) is in agreement with the results of the TEM analysis while those obtained from the other two models are significantly varied. Thus it may be concluded that the uniform deformation energy model is more realistic in the present case. This is in agreement with the results of Rosenberg et al. that for metallic samples with cubic structures the uniform deformation energy model is suitable [11].

The RMS lattice strain $\langle e_{RMS}\rangle = (2/\pi)^{1/2}(\Delta d/d_0)$ [14] estimated from observed variation in the interplanar spacing values are plotted against those estimated using uniform deformation energy density model, ε_{hkl} is plotted in Fig. 5. Here d and d_0 represents the observed and ideal interplanar spacing values respectively. The straight line in Fig. 5 serves as a guide for the eye. Ideally, if the estimations from both the estimations are exactly in agreement all the points should lie on a straight line making an angle

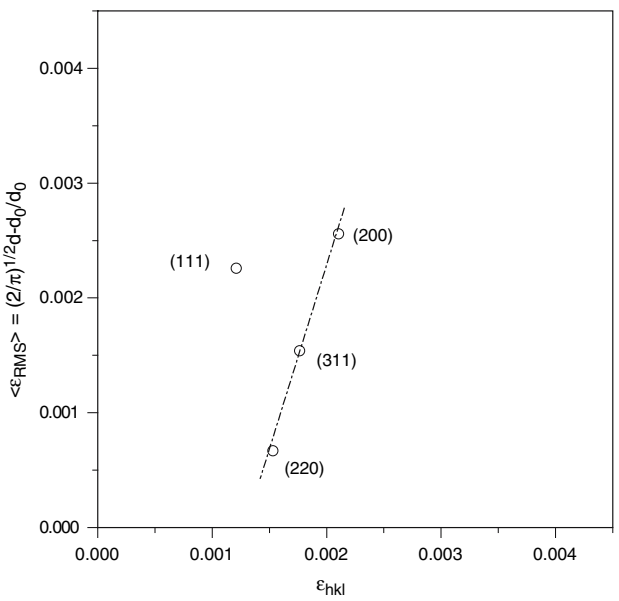

Fig. 5 RMS lattice strain estimated from interplanar spacing values plotted against lattice strain obtained from uniform deformation energy density model. The straight line serves as a guide for the eye

45° with the *X*-axis. However, such an agreement cannot be expected since the *X*-axis data are determined by the analysis of X-ray diffraction peak widths while the *Y*-axis data are determined from the positions of the peaks. The numerical values obtained from the two different routes lie in the range 0.0007 and 0.003 are compatible with each other except for the discrepancy along [111] direction (space diagonal). The discrepancy along [111] direction is probably due to the greater stiffness in this direction [11]. Further, the numerical values of strain obtained from both the measurements are comparable to those reported for FCC metal nanoparticles of comparable particle size [15].

Lattice strain in nanocrystalline sample may arise from the excess volume of grain boundaries [1] and/or due to dislocations [4–6]. Recently, Quin and Szpunar [1] had suggested a model for estimating lattice strain due to excess volume of grain boundaries associated with vacancies and vacancy clusters. An estimation of lattice strain for silver nanoparticles with average crystallite size of $\sim$50 nm using this model results in values which are about one-tenth of the experimentally observed values. This points to the possibility that the lattice strain in nanocrystalline Ag samples of the present study has considerable contribution from dislocations, which are located at the grain boundaries. This argument is supported by earlier reports that in nanocrystalline metal samples there is a possibility of deviations from ideal lattice sites within $\sim$2–3 monolayers of the grain boundaries [15]. Thus, the most significant contribution to the lattice strain in nanocrystalline Ag sample of the present study is from dislocations.

Conclusion

In summary, X-ray diffraction pattern of nanocrystalline silver with an average particle size of about 51 $\pm$ 8 nm was recorded. The size and strain contributions to line broadening were analysed by the method of Williamson and Hall using uniform deformation, uniform deformation stress and uniform deformation energy density models. Uniform deformation energy density model models the strain most appropriately. The anisotropic lattice strain values estimated from the observed variation in the interplanar spacing values and those estimated using uniform energy density models are in agreement with each other. The numerical value of lattice strain is about 10 times larger than that estimated using the model suggested by Quin and Szpunar, which traces the origin of lattice strain to the stress filed due to the excess volume of grain boundaries, associated with vacancies and vacancy clusters. The most significant contribution to the lattice strain in nanocrystalline Ag sample of the present study is from dislocations.

References

1. Quin W, Szpunar JA (2005) Phil Mag Lett 85:649
2. Zhao YA, Lu K (1997) Phys Rev B 56:14330
3. Lu K, Sui ML (1995) Acta Metall Mater 43:43
4. Eckert J, Holzer JC, Krill CE (1992) J Mater Res 7:1751
5. Hellstorm E, Fecht HJ, Fu Z (1989) J Appl Phys 65:305
6. Nazrov AA, Romanov AE, Valiev RR (1994) Nanostruct Mater 4:93
7. Zorn G (1988) Aust J Phys 41:237
8. Chipara SJ, Bish DL (1991) Adv X-ray Anal 34:473
9. Wiliamson GK, Hall WH (1953) Acta Meatall 1:22
10. Klug HP, Alexander LE (1974) In: X-ray diffraction procedure for polycrystalline and amorphous materials. Wiley, New York
11. Rosenberg Yu, Machavariant VSh, Voronel A, Garber S, Rubshtein A, Frenkel AI, Stern EA (2000) J Phys: Condens Mater 12:8081
12. Love AEH (1944) In: A treatise on the mathematical theory of elasticity. Dover, New York
13. Landollt-Börnstein New Series 1979, vol 11. Springer, Berlin
14. Dapiaggi M, Geiger CA, Artioli G (2005) Am Miner 90:506
15. Oleszak D, Shingu PH (1996) J Appl Phys 79:2975